

Molecular signatures of basal cell carcinoma susceptibility and pathogenesis: A genomic approach

ELIZABETH ROSE HELLER^{1*}, ANKIT GOR^{1*}, DAN WANG², QIANG HU², ALBERTA LUCCHESI³, DARJA KANDUC⁴, MEENA KATDARE⁵⁻⁷, SONG LIU² and ANIMESH A. SINHA¹

¹Department of Dermatology, State University of New York at Buffalo and Roswell Park Cancer Institute;

²Department of Biostatistics, Roswell Park Cancer Institute, Buffalo, NY, USA; ³Department of Odontostomatological, Orthodontics, and Surgical Disciplines, Faculty of Medicine, Second University of Naples (SUN), Naples;

⁴Department of Biochemistry and Molecular Biology, University of Bari, Italy; ⁵Department of Surgery, Carcinogenesis and Chemoprevention Laboratory, Weill Medical College of Cornell University, New York, NY; ⁶Skin of Color Research Institute, Hampton University, Hampton, VA; ⁷Department of Dermatology and Leroy T. Canoles Jr Cancer Research Center, Eastern Virginia Medical School, Norfolk, VA, USA

Received September 2, 2012; Accepted October 22, 2012

DOI: 10.3892/ijo.2012.1725

Abstract. Gene expression profiling can be useful for phenotypic classification, investigation of functional pathways, and to facilitate the search for disease risk genes through the integration of transcriptional data with available genomic information. To enhance our understanding of the genetic and molecular basis of basal cell carcinoma (BCC) we performed global gene expression analysis to generate a disease-associated transcriptional profile. A gene signature composed of 331 differentially expressed genes (DEGs) was generated from comparing 4 lesional and 4 site-matched control samples using Affymetrix Human Genome U95A microarrays. Hierarchical clustering based on the obtained gene signature separated the samples into their corresponding phenotype. Pathway analysis identified several significantly overrepresented pathways including PPAR- γ signaling, TGF- β signaling and lipid metabolism, as well as confirmed the importance of SHH and p53 in the pathogenesis of BCC. Comparison of our microarray data with previous microarray studies revealed 13 DEGs overlapping in 3 studies. Several of these overlapping genes function in lipid metabolism or are components of the extracellular matrix, suggesting the importance of these and related pathways in BCC pathogenesis. BCC-associated DEGs were mapped to previously reported BCC susceptibility loci

including 1p36, 1q42, 5p13.3, 5p15 and 12q11-13. Our analysis also revealed transcriptional 'hot spots' on chromosome 5 which help to confirm (5p13 and 5p15) and suggest novel (5q11.2-14.3, 5q22.1-23.3 and 5q31-35.3) disease susceptibility loci/regions. Integrating microarray analyses with reported genetic information helps to confirm and suggest novel disease susceptibility loci/regions. Identification of these specific genomic and/or transcriptional targets may lead to novel diagnostic and therapeutic modalities.

Introduction

Basal cell carcinoma (BCC) is the most common malignancy among Caucasians, with a rising estimated yearly incidence of 2.75 million cases worldwide (1). BCC is more common among elderly men, with a peak incidence after the age of eighty. Individuals with a fair phenotype, including red or blonde hair and light eyes, are particularly at risk. While BCC can develop on any skin surface, the majority of lesions appear on the head and neck. Based on their histological and clinical features, BCC can be classified into one of several types including nodular, superficial, morpheaform, nevoid, and pigmented (2). Nodular BCC is the most common subtype, comprising 21% of all cases (3). Although BCC is slow-growing and rarely metastasize, it is locally invasive and thus may cause extensive damage to surrounding tissue. Despite effective treatment via local excision, tumor recurrence is relatively common at 1-10% (4).

Despite its high prevalence, the etiopathogenesis of BCC is still unclear. Previous studies have indicated a multifactorial, polygenic basis for disease. The current model for BCC pathogenesis maintains that UV radiation causes DNA damage in exposed cells. If this damage goes unrepaired, the resulting oncogene-activating or tumor suppressor-inactivating mutations allow cells to bypass cell cycle regulation and thus undergo uncontrolled proliferation. The role of UV damage in BCC pathogenesis is further indicated by the predominant location of

Correspondence to: Professor Animesh A. Sinha, Department of Dermatology, University at Buffalo and Roswell Park Cancer Institute, Buffalo, NY 14263, USA
E-mail: aasinha@buffalo.edu

*Contributed equally

Key words: basal cell carcinoma, microarray, non-melanoma, skin cancer, pathogenesis, genetics, tumor, gene expression

BCC on sun-exposed surfaces, as well as the presence of 'UV signature' mutations (i.e., T → C transversions) in affected cells (5,6). Other exposures that can predispose to carcinogenesis are those to arsenicals, polyaromatic hydrocarbons, immunosuppression, and psoralen therapy (2).

Studies have identified several somatic mutations associated with the development of BCC (2,5,7-9). Of note, the presence of mutations in the Patched-1 (PTCH-1) gene has helped elucidate the role of the sonic hedgehog (SHH) signaling pathway in pathogenesis. PTCH-1 is an inhibitor of the protein Smoothed (SMO), whose role is to activate the transcription of cell cycle regulators like WNT5A. When PTCH-1 activity is lost, SMO is constitutively activated, allowing uncontrolled cell proliferation to take place (5). A loss of function mutation in P53 has also frequently been associated with BCC as well as many other cancers (6,10). P53 encodes the protein p53, an established tumor suppressor. This protein causes cell cycle arrest in the presence of DNA damage, thereby preventing the replication of damaged genetic material and allowing either DNA repair or apoptosis to take place.

Genome-wide association studies (GWAS) have been instrumental in identifying several loci that confer susceptibility to BCC. These studies report loci associated with BCC and pigmentation genes (SLC45A2, TYR, MC1R, ASIP) as well as loci associated with BCC alone (PADI6, RHOU, KLF14, KRT5, TERT/CLPTMIL). These results support the conclusion that both pigmentation-independent and pigmentation-dependent pathways exist in the development of BCC. Although genomic studies and linkage analyses provide a framework for identifying putative loci, they do not address the gene expression that underlies disease pathogenesis.

In this study, we employed microarray analysis to determine a molecular profile for BCC which was then used to i) classify samples based on phenotype via hierarchical clustering methods, ii) identify significantly enriched pathways important to BCC pathogenesis, and iii) integrate genetic information with our transcriptional data in order to identify potential genetic risk factors. Specifically, we obtained a list of differentially expressed genes (DEGs) from a comparison of lesional vs. site-matched non-lesional skin samples from patients with a confirmed diagnosis of nodular basal cell carcinoma. Pathway analysis of the resulting DEGs identified multiple dysregulated functional pathways, including those involved in PPAR- γ signaling, TGF- β signaling, and lipid metabolism. A comparison of our list of DEGs to molecular profiles in published studies identified several overlapping genes and pathways of interest in BCC. We further compared the chromosomal locations of our list of DEGs with reported genomic susceptibility loci to focus the search for genes of pathogenetic significance. Furthermore, our analysis identified potential transcriptional 'hot spots' in which there is an enhanced correlation of significantly altered gene expression at particular chromosomal locations, areas which may be of particular interest for future genetic studies. By integrating transcriptional data with genomic information, our study reveals potential susceptibility loci/regions associated with BCC in terms of altered gene expression. Detailed characterization of the genetic and transcriptional alteration associated with BCC development may lead to novel therapeutic modalities based on specific genomic and/or transcriptional targets.

Materials and methods

Patient recruitment and tissue handling. The study was approved by the Institutional Review Board of Weill-Cornell Medical College of Cornell University/New York Presbyterian Hospital (IRB # 0998-398). Subjects diagnosed with BCC based on established clinical and histological criteria were recruited through the dermatology outpatient clinic of New York Presbyterian Hospital. Informed consent was obtained from all study subjects before 6 mm punch biopsies were performed and collected. In total, 8 biopsies (4 lesional and 4 site-matched non-lesional) were used for gene expression analysis of skin from BCC patients. Specimens were snap frozen in liquid nitrogen immediately following sampling for subsequent RNA extraction. Demographic information, duration of disease and treatment history were obtained from each subject at the time of sampling (see Table I for details on samples and patients).

RNA extraction and cRNA production. Total RNA was isolated using TRIzol reagent (Invitrogen Corp., Carlsbad, CA) following the manufacturer's protocol. RNA was subsequently purified using an RNeasy Mini Kit (Qiagen Inc., Valencia, CA). A cDNA template was synthesized from 16 μ g of total RNA from each sample, and then used for biotinylated cRNA generation.

Microarray analysis. Fragmented cRNA was hybridized to Human Genome U95Av2 microarrays (Affymetrix Inc., Santa Clara, CA) for 16 h at 45°C. The chips were then washed, stained and scanned according to manufacturer's protocol (Affymetrix Inc.). The U95Av2 chip contains almost 63,000 probe sets representing approximately 54,000 UniGene clusters and over 10,000 full-length genes (http://media.affymetrix.com/support/technical/datasheets/made_datasheet.pdf).

The resulting data were analysed using the Bioconductor packages in the R statistical computing environment for data processing (11). For data quality control, we used the Simpleaffy package to remove samples that failed in a variety of QC metrics for assessing the RNA quality, sample preparation and hybridization (12). This led to 8 samples for further microarray data analysis. The MAS5.0 function was used to generate expression summary values, followed by trimmed mean global normalization to bring the mean expression values of all eight arrays to the same scale. Then, we filtered out the genes whose expression-status was called absent (i.e., indistinguishable from the background intensity) across >50% of both tumor and normal groups. About 5,918 genes passed the quality filtering for downstream analysis.

We then performed the comparisons between tumor group and normal group. We used the Limma program in the Bioconductor package to calculate the level of gene differential expression (13). Briefly, a linear model with paired design matrix was fit to the data. The false discovery rate approach of Benjamini and Hochberg was used to adjust multiple comparisons (14). At the FDR of 0.1, we obtained the list of differentially expressed genes (DEGs) with at least 2-fold changes.

Following single gene-based significance testing, we used the expression value of DEGs to cluster the patients. Our purpose was to determine whether the identified DEGs were able to serve as a gene signature to classify samples into their corres-

Table I. Demographic data for study participants.

Patient	Age	Gender	Ethnicity	Diagnosis	Duration	Location-lesional	Location-non-lesion
1003	75	M	Caucasian	BCC-nodular	3 years	Right back	Right back
1008	86	M	Caucasian	BCC-nodular	4 months	Left cheek	Left cheek
1053	65	M	Caucasian	BCC-nodular	Unknown	Left periauricular	Left periauricular
1055	Unknown	M	Caucasian	BCC-nodular	Unknown	Face	Face

Table II. Enriched canonical pathways in the differentially expressed genes (DEGs) obtained from the comparison of lesional versus site-matched, non-lesional samples using DAVID and Pubmed literature searches.

Pathway name	DEGs counts	P-value
hsa4510: focal adhesion ^b	19	0.000250723
hsa4512: ECM-receptor interaction ^a	16	9.85082E-08
hsa3320: PPAR signaling pathway	11	2.28729E-06
hsa4350: TGF-beta signaling pathway	7	0.0415292
hsa900: terpenoid backbone biosynthesis ^b	6	2.28729E-06
hsa280: valine, leucine and isoleucine degradation	6	0.005172845
hsa71: fatty acid metabolism	5	0.017984405
hsa100: steroid biosynthesis ^a	5	0.000298256
hsa1040: biosynthesis of unsaturated fatty acids	5	0.004048771
hsa260: glycine, serine, and threonine degradation	4	0.068063005
hsa650: butanoate metabolism	4	0.084866208

^aDenotes a pathway common to Howell *et al* (18) and our study; ^bdenotes a pathway overlapping Howell *et al* (18), O'Driscoll *et al* (19), Asplund *et al* (17) and our study).

ponding phenotype groups. A hierarchical clustering algorithm based on the average linkage of Pearson Correlation was employed (15). Pathway analysis was performed using NIH DAVID Tools (16). The statistical significance was calculated using the Hypergeometric test in which the null hypothesis is that no difference exists between the number of genes falling into a given pathway in the target DEG list and the genome as a whole. A list of enriched KEGG pathways with p-values <0.05 and including at least 4 genes was kept.

Results

Hierarchical clustering separates samples by disease status. A total of 8 skin biopsies from patients with nodular BCC, lesional (n=4) and non-lesional (n=4), were analysed using Affymetrix Human Genome U95A2 microarray chips (Affymetrix) to generate gene expression profiles (see Table I for details on samples and patients). We performed the comparison of expression profiles between the tumor and normal groups. At the false discovery rate of 0.1, we identified a total of 331 differentially expressed genes (DEGs) with at least 2-fold expression changes. 144 DEGs are upregulated (fold changes ranging from +2.0 to +53.1) in the tumor group while 187 genes are downregulated (fold changes ranging from -2.0 to -32.7). Hierarchical

clustering of obtained DEGs was performed, which separates the 8 samples into their corresponding phenotype groups (Fig. 1).

Functional analysis reveals dysregulation of genes involved in multiple pathways. To explore the key biological processes altered in the tumor vs non-tumor control samples, we performed enrichment tests to identify the significantly overrepresented canonical pathways among the differentially expressed genes. Functional annotation and pathway analysis were performed using the database for annotation, visualization, and integrated discovery (DAVID) and Pubmed literature searches (Table II). The pathways enriched in the differentially expressed genes include cell-cell interactions such as focal adhesion (19 genes) and ECM-receptor interaction (16 genes), PPAR signaling pathway (11 genes) and TGF- β signaling pathway (7 genes), terpenoid backbone biosynthesis (6 genes), and fatty acid metabolism (5 genes). Our analysis revealed, with the exception of one gene (MMP-1), the downregulation of DEGs falling within the PPAR- γ signaling pathway. The downregulation was also seen in DEGs involved in fatty acid metabolism, and terpenoid backbone biosynthesis. Additionally, the DEGs pertaining to focal adhesion and cell-cell interactions are mostly upregulated, with the exception of one gene (ITGA7) (Fig. 2).

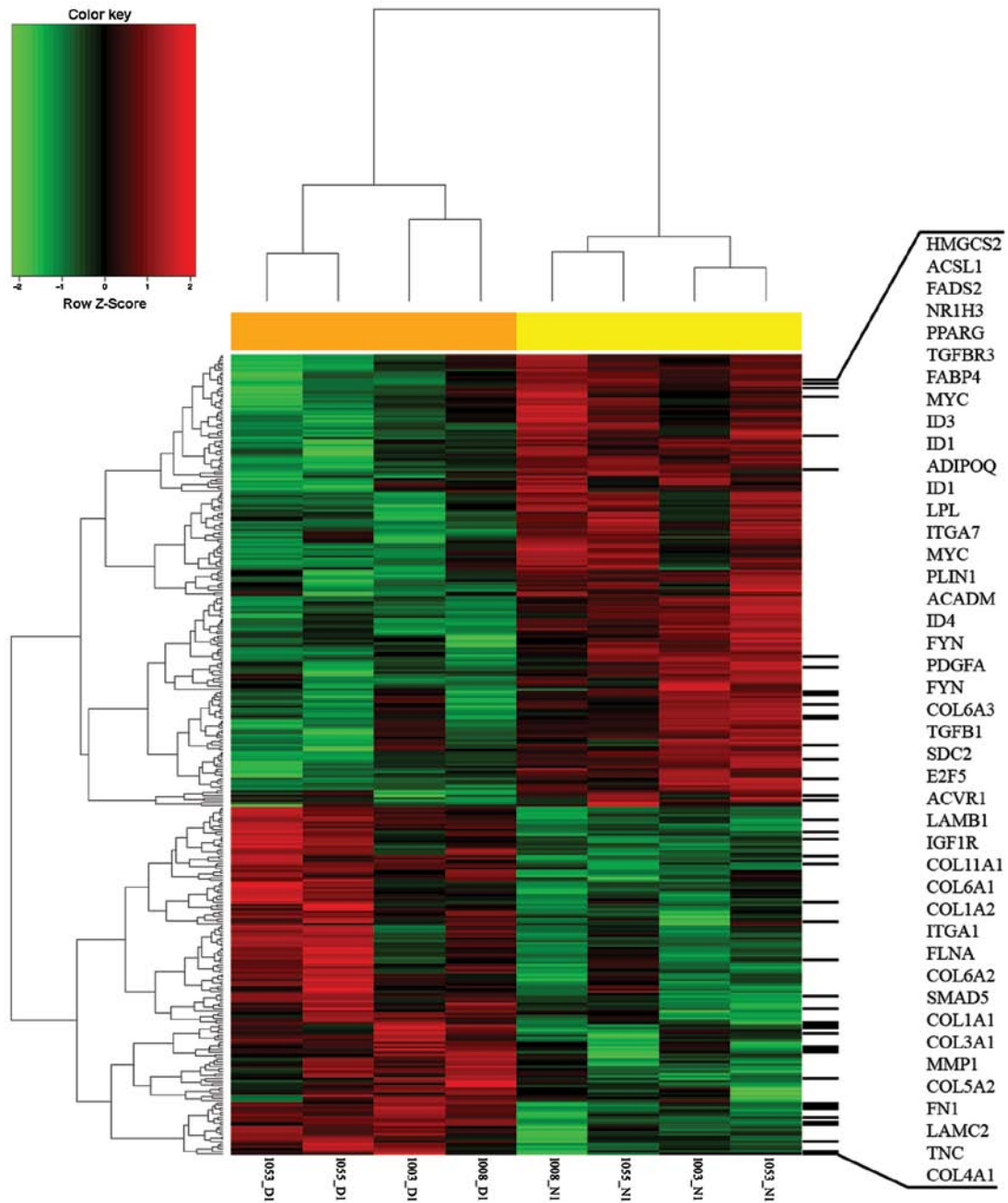


Figure 1. Hierarchical clustering of samples based on DEGs with at least 2-fold change and controlled by false discovery rate of 0.1, as inferred from disease versus matched normal samples. In the clustering heat map, red indicates upregulation while green indicates downregulation. In the sample clustering dendrogram, orange indicates disease (lesional) samples while yellow indicates control (site-matched non-lesional) samples. Select genes are listed on the right.

Comparison of DEGs across microarray studies reveals overlapping genes/pathways of interest. To evaluate potential consensus genes associated with BCC pathogenesis, we compared our list of DEGs to four previously published microarray studies regarding gene expression in BCC (17-20). In our analysis, we excluded Yu *et al* due to significant methodological differences. Specifically, the authors compared molecular profiles between different BCC subtypes and not between tumor (without subtype distinction) and normal skin. We first examined data from Howell *et al*, as their study used site-matched non-lesional samples as controls (Table III, second left-most column). Comparing our data to a similarly

conducted study allowed us to minimize the presence of potentially confounding experimental design and technical variances. Twenty-six DEGs were found to overlap between our study and Howell *et al*; 8 genes were upregulated in the same direction (MDK, LUM, COL4A1, CDH11, DUSP10, COL5A2, STAT1, and SDC2), 14 genes were downregulated in the same direction (NR4A1, CYB5A, APOC1, DHCR24, PLA2G2A, FDPS, PPARG, ADH1B, HMGCR, DUSP1, PLA2G7, LPL, FABP4, and ALDH1A1) and 4 genes were differentially expressed in opposite directions (UBE2D1, KRT7, KRT18 and DAPK1). Pathway analysis revealed genes that were differentially expressed in processes such as PPAR- γ signaling,

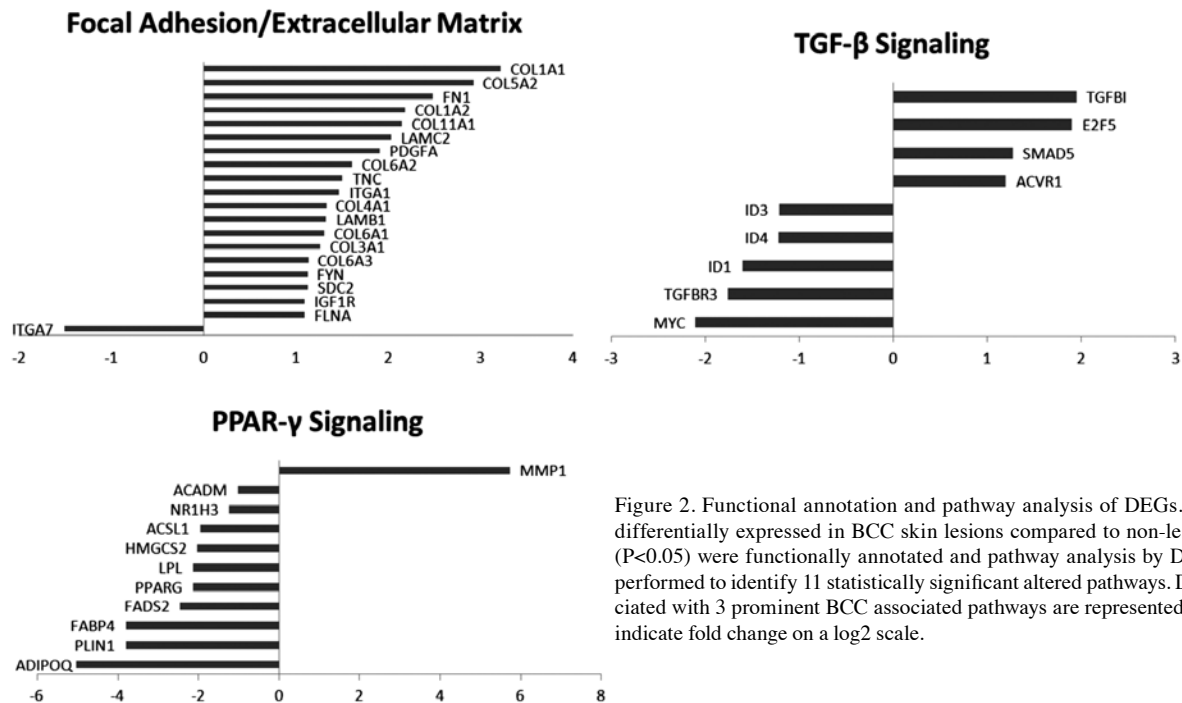


Figure 2. Functional annotation and pathway analysis of DEGs. 331 genes differentially expressed in BCC skin lesions compared to non-lesional skin ($P < 0.05$) were functionally annotated and pathway analysis by DAVID was performed to identify 11 statistically significant altered pathways. DEGs associated with 3 prominent BCC associated pathways are represented here. Bars indicate fold change on a log2 scale.

cell-cell interaction, terpenoid backbone biosynthesis, and MAPK signaling.

We also compared our data more broadly with combined data from Howell *et al* (18) as well as with O'Driscoll *et al* (19), and Asplund *et al* (17), disregarding certain methodological differences. A total of 1842 DEGs were compared and 193 genes were found to overlap with at least one other study (Table III). 186 DEGs were dysregulated in the same direction (100 upregulated and 86 downregulated) while 7 genes were differentially expressed in opposite directions (FOSB, CYR61, DICER1, UBE2D1, KRT7, KRT18 and DAPK1). Pathway analysis of these DEGs revealed a dysregulation of the genes involved in focal adhesion, extracellular matrix-receptor interaction, terpenoid backbone biosynthesis, and steroid biosynthesis, which overlapped with a large number of pathways derived from analysis of our DEGs. Thirteen DEGs overlapped across three studies, including our own (Table IV). Functional annotation and pathway analysis revealed that 5 of the 13 DEGs were involved in either cell-cell interaction or terpenoid backbone biosynthesis.

DEGs and transcriptional 'hot spots' map to several genetic susceptibility loci/regions. We have mapped chromosomal locations for the top 20 upregulated and downregulated DEGs identified in our study (Table V). We then compared chromosomal locations of DEGs with putative BCC susceptibility loci previously reported in genome-wide association and linkage studies, as well as regions where somatic mutations, determined either in human subjects or murine models, have been implicated in the pathophysiology of BCC (Table VI). A total of 62 DEGs, 25 upregulated and 37 downregulated, were mapped to these regions.

Next, we examined our gene expression data to identify chromosomes with a significant enrichment of DEGs. A statis-

tically significant over-representation of DEGs was found on chromosome 5 (odds ratio=1.65, $P=0.025$) (Fig. 3). The location of DEGs within chromosome 5 includes 5p13-15.33, 5q11.2-14.3, 5q22.1-23.3, and 5q31-35.3 (Fig. 4), which contain 22 DEGs (12 upregulated, 10 downregulated). The transcriptional 'hot spots' on 5p13 and 5p15 were also identified in recent BCC genome-wide association studies. The 5q11.2-14.3, the 5q22.1-23.3 and the 5q31-35.3 regions represent novel chromosomal locations with potential relevance to BCC that may warrant further genetic investigation.

Discussion

Although BCC has been investigated at both the genetic and transcriptional levels, many details related to pathogenetic events remain unknown. To help elucidate the links between the genetic factors and altered gene expression that impact tumor development, we performed gene expression analysis to define a BCC associated transcriptional profile.

Our analysis was conducted using 8 samples, with 4 lesional samples and 4 site-matched non-lesional controls. We utilized a site-matched, pair-wise study design to eliminate variance due to differences in gene expression between individuals. This approach allowed us to focus directly on transcriptional alterations between tumor and non-tumor tissues without the aforementioned confounding variables. Further studies investigating differences between non-lesional skin in patients with BCC and skin of healthy individuals may provide additional insight into underlying genetic contributions to BCC. While differences in sample preparation, sample type, microarray platform, and analytical software present complicating factors in comparative analysis, our results do overlap with several DEGs reported in three previous microarray studies (Tables III and IV).

Table III. List of DEGs overlapping with at least one other study. DEGs are organized by gene expression in the same or opposite direction.

	Howell <i>et al</i> (18)	O'Driscoll <i>et al</i> (19)	Asplund <i>et al</i> (17)	Total
Total no. of DEGs investigated	249	3922	361	4521
No. of overlapping DEGs (up, down, opposite directions)	26 (8, 14, 4)	149 (80, 66, 3)	18 (12, 6, 0)	193 (100, 86, 7)
Overlapping DEGs upregulated in the same direction	MDK LUM COL4A1 CDH11 DUSP10 COL5A2 STAT1 SDC2	HTRA1 MDK MICAL2 TSPAN4 SSPN RECQL DYRK2 ZFC3H1 LUM PLXNC1 COL4A1 SLC7A8 DIO2 CHGA SH3GL3 CSPG4 IGF1R CDH3 CDH11 CDH13 TOP2A VEZF1 BPTF SLC16A3 EMP3 COL11A1 LRP8 PHC2 MARCKSL1 STMN1 MFAP2 GPR161 LAMC2 DUSP10 PARP1 NID1 CEP170 NINL COL6A2 MMP11	SFRS7 MYCN MYO1B COL5A2 ACVR1 FN1 COL6A3 WNT5A SLCO2A1 CHST2 SHOX2 ADAMTS3 BASP1 LPCAT1 F2R TNPO1 VCAN C5orf13 TGFB1 DBN1 TRAM2 SOX4 AEBP1 PDGFA CALD1 SLC39A14 LOXL2 TUSC3 SDC2 NFIB PTCH1 TNC DAPK1 TRO MAGED1 AP1S2 HEPH TMSB15A FLNA BGN	GPR161 SOX4 ACVR1 BASP1 CHST2 DYRK2 LAMB1 NFIB SPARC SHOX2 SDC2 TUSC3
Overlapping DEGs down- regulated in the same direction	NR4A1 CYB5A APOC1 DHCR24 PLA2G2A FDPS PPARG ADH1B HMGR	AKR1C1 AKR1C2 AKR1C3 IDI1 C10orf116 ALDH3B2 DHCR7 GAL EXPH5	BTG2 CHI3L GNPAT C2CD2 TST HIBCH TKT	ABCC3 FCGBP ALOX15B GHR MGST2 NTRK2

Table III. Continued.

	Howell <i>et al</i> (18)	O'Driscoll <i>et al</i> (19)	Asplund <i>et al</i> (17)	Total
	DUSP1	CRYAB	ABHD5	
	PLA2G7	ZBTB16	MGST2	
	LPL	ITGA7	SC4MOL	
	FABP4	ENDOU	ACSL1	
	ALDH1A1	METTTL7A	HMGCS1	
		EFNB2	PAPD7	
		CKB	SRD5A1	
		CA12	HMGCR	
		MEF2A	WWC1	
		SHMT1	ELOVL5	
		ACADVL	CDKN1A	
		ALOX15B	PLA2G7	
		TOB1	FKBP5	
		ABCC3	ID4	
		ABCA8	GPR126	
		OSBPL1A	COBL	
		CYB5A	AZGP1	
		LDLR	INSIG1	
		ECH1	FABP4	
		BLVRB	MYC	
		DHCR24	PLIN2	
		TGFBR3	NTRK2	
		PMVK	CRAT	
		FDPS	EBP	
			MAOA	
			NSDHL	
Overlapping DEGs expressed in opposite directions	UBE2D1 KRT7 KRT18 DAPK1	FOSB CYR61 DICER1		

Hierarchical clustering of obtained DEGs revealed that samples could be distinguished by disease status, with disease and control samples separating into discrete groups. The establishment of a BCC tumor expression signature may be useful for the development of molecular diagnostic modalities in BCC, and extended transcriptional profiles could allow classification of newly diagnosed BCC into specific subtypes (i.e. nodular, morpheaform, and superficial) as an addition to standard clinical and pathological criteria. In the future, it may be possible to classify patients into subgroups according to predicted therapeutic efficacy or risk of recurrence, thereby improving patient outcomes.

Functional analysis of our data revealed transcriptional dysregulation in multiple pathways affecting PPAR- γ signaling, lipid metabolism, TGF- β signaling, cell-cell interactions, as well as many others, with intriguing implications regarding cancer pathogenesis and localizing potential therapeutic targets. For example, recent research into the PPAR- γ signaling has elucidated its role in a variety of cellular processes. PPAR- γ is a receptor whose ligands include steroid, hormones, and retinoids (21-23). Once activated, PPAR- γ dimerizes with the retinoid X receptor to activate transcription of genes involved

in lipid metabolism and differentiation. In our study, there was a downregulation of PPAR- γ as well as its transcriptional target genes (ADIPOQ, FABP4, PLIN1, LPL, ACS, NR4A1, FADS2, HMGCS1), indicating aberrant PPAR- γ signaling in our samples. Our analysis also revealed transcriptional dysregulation in pathways regarding lipid metabolism, unsaturated fatty acid biosynthesis, steroid biosynthesis as well as terpenoid backbone biosynthesis. Whether these processes are a cause or consequence of PPAR- γ signaling dysregulation remains to be determined.

Interestingly, the PPAR- γ signaling pathway has been implicated in a variety of cancers, including, but not limited to, bladder cancers, colon cancers, squamous cell carcinomas and melanomas (21,22,24-26). PPAR- γ has been shown to be down-regulated in certain tumors (27,28); however, other studies have shown an upregulation of PPAR- γ in other malignancies (29-31). These discrepancies warrant further investigation on the role of PPAR- γ in specific tumors. PPAR- γ activation has been implicated in reducing cell proliferation and/or inducing apoptosis in a wide array of cancer cell lines. *In vitro* studies on lung cancer cell lines have shown that PPAR- γ activation acts to reduce cell growth by promoting differentiation (32). Some

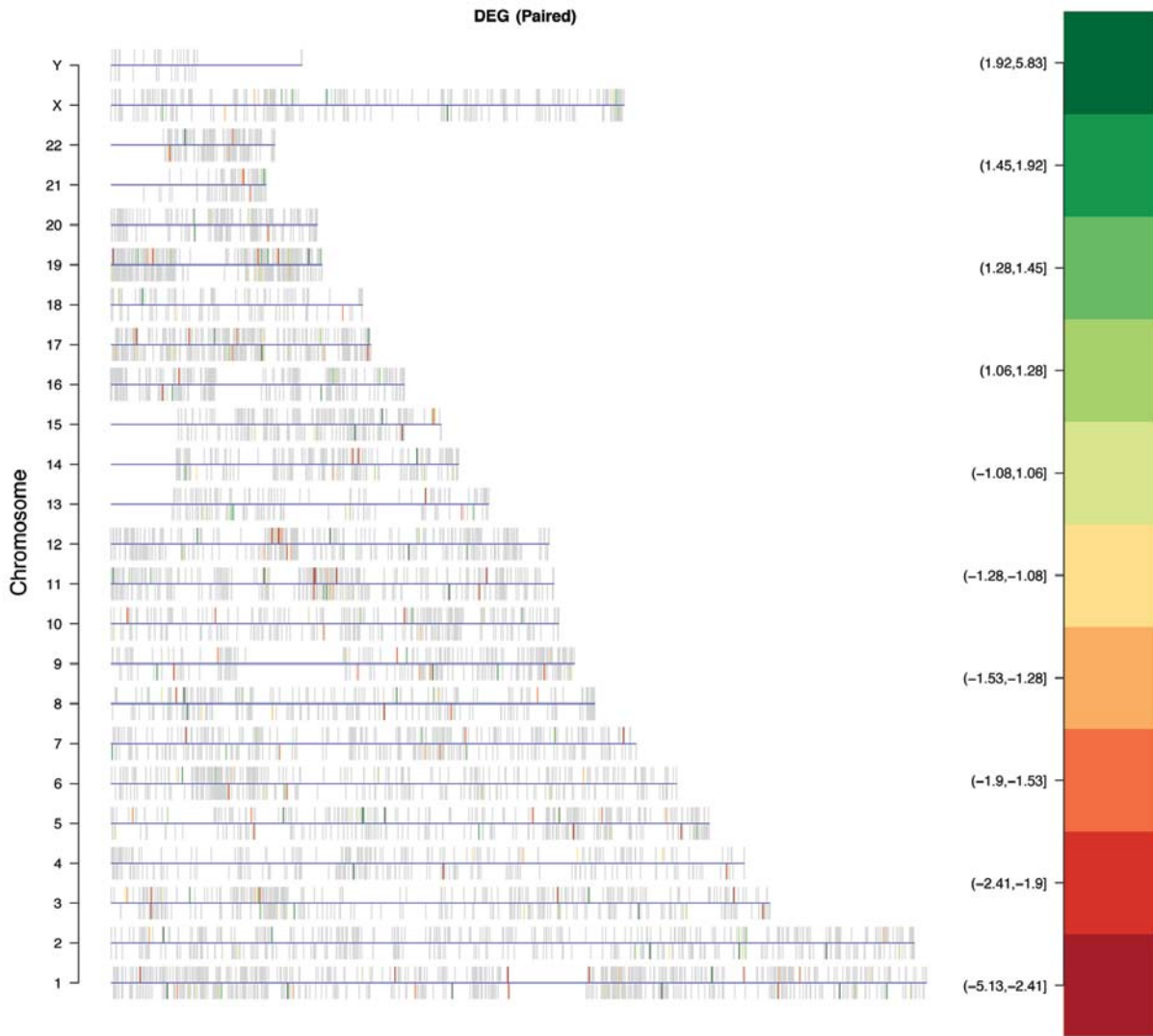


Figure 3. The genome-wide chromosomal distribution of DEGs with at least 2-fold change and controlled by false discovery rate of 0.1, as inferred from disease versus matched normal samples. Each horizontal line corresponds to one chromosome. Genes are represented by short vertical lines which go up if the gene is on the sense strand and down if it is on the anti-sense strand. The identified DEGs are found to be enriched on chromosome 5 (odds ratio=1.65, $P=0.025$).

transcriptional target genes have been identified as prognostic factors for certain tumors. Of note, fatty acid binding protein 4 (FABP4) expression has been shown to correlate with bladder cancer progression (33). FABP4 plays a role in signal transduction, affects glucose and lipid metabolism, and potentiates apoptosis (34). Decreased levels of FABP4 denoted a worse prognosis in patients with bladder tumors. Our study revealed a decreased expression of FABP4. Future studies may indicate if transcriptional levels of FABP4 can be used as an indicator of cancer progression in basal cell carcinoma.

Although transcriptional dysregulation of the PPAR signaling pathway has been established in a variety of tumors, our study represents aberrant signaling in basal cell carcinomas. The PPAR- γ signaling pathway represents an intriguing therapeutic target, as PPAR- γ activation via pharmaceuticals has been used in studies to investigate cancer treatment. *In vitro* use of thiazolidinediones (TZD), such as rosiglitazone and troglitazone, demonstrated anti-proliferative, pro-apoptotic, and differentiation-promoting effects (21,26). Future experi-

ments using PPAR- γ agonists on mouse models as well as BCC cell lines may elucidate more clues on the pathogenesis of the disease and help develop novel therapeutic options for patients with basal cell carcinoma.

Our data confirm certain well-established genetic mechanisms underlying BCC pathogenesis. The sonic hedgehog (Shh) signaling pathway is often cited as an important player in disease development (2,5,7,8). Several genes in the Shh pathway can be found amongst the DEGs in our list. Our analysis revealed the upregulation of PTCH-1, a primary mediator of the Shh pathway. When not bound by Shh, PTCH-1 inhibits Smoothed, thus preventing signal transduction and transcription of downstream target genes. Among these target genes are PTCH-1 for negative feedback, GLI1 for positive feedback, WNT5A, a gene involved in differentiation, and MYCN, a gene associated with the development of neuroblastomas. When inhibition of Smoothed is lost due to mutation, transcription of target genes can occur constitutively and therefore promote disease initiation and progression (35). Given that our results

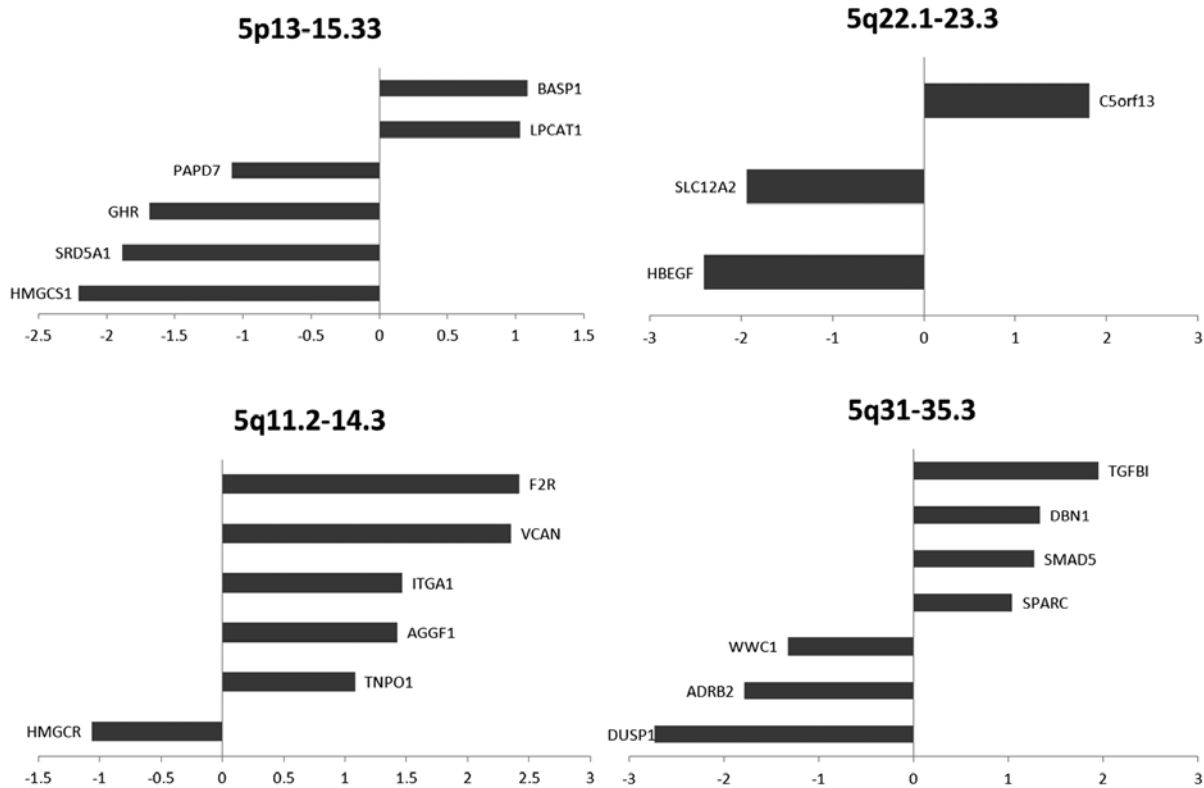


Figure 4. DEGs within transcriptional 'hot spots'. Differentially expressed genes within transcriptional 'hot spots' in patients with BCC were annotated by chromosomal location. Bars indicate fold change on a log₂ scale.

Table IV. DEGs overlapping across 3 studies [this study; Howell *et al*, 2005 (18); O'Driscoll *et al*, 2006 (19)].

Gene symbol	Entrez gene	Gene title	Chromosomal location	Fold change
MDK	4192	Midkine (neurite growth-promoting factor 2)	chr11p11.2	1.669
LUM	4060	Lumican	chr12q21.3-q22	1.925
COL4A1	1282	Collagen, type IV, alpha 1	chr13q34	1.333
CDH11	1009	Cadherin 11, type 2, OB-cadherin (osteoblast)	chr16q22.1	1.740
DUSP10	11221	Dual specificity phosphatase 10	chr1q41	2.222
COL5A2	1290	Collagen, type V, alpha 2	chr2q14-q32	2.926
SDC2	6383	Syndecan 2	chr8q22-q23	1.128
DAPK1	1612	Death-associated protein kinase 1	chr9q34.1	1.355
DHCR24	1718	24-dehydrocholesterol reductase	chr1p33-p31.1	-1.407
FDPS	2224	Farnesyl diphosphate synthase (farnesyl pyrophosphate synthetase, dimethylallyltranstransferase, geranyltranstransferase)	chr1q22	-1.460
HMGCR	3156	3-hydroxy-3-methylglutaryl-CoA reductase	chr5q13.3-q14	-1.063
PLA2G7	7941	Phospholipase A2, group VII (platelet-activating factor acetylhydrolase, plasma)	chr6p21.2-p12	-1.103
FABP4	2167	Fatty acid binding protein 4, adipocyte	chr8q21	-3.797

Fold changes are provided in log₂ scale.

reveal upregulation of PTCH1, WNT5A, and MYCN, this constitutive activation seems likely. Additionally, several DEGs share the same chromosomal locations as established genes of

interest in BCC pathogenesis such as PTCH1, SUFU, PTCH2, and Gli2 (Table VI), thus reinforcing their putative role as genetic susceptibility loci.

Table V. The 20 most A) upregulated and B) downregulated genes.

A)				
Gene symbol	Entrez gene	Gene title	Chromosomal location	Fold change
MMP1	4312	Matrix metalloproteinase 1 (interstitial collagenase)	chr11q22.3	53.059
CHGA	1113	Chromogranin A (parathyroid secretory protein 1)	chr14q32	32.067
MYCN	4613	v-myc myelocytomatosis viral related oncogene, neuroblastoma derived (avian)	chr2p24.1	16.000
LRP8	7804	Low density lipoprotein receptor-related protein 8, apolipoprotein e receptor	chr1p34	12.502
ADAMTS3	9508	ADAM metalloproteinase with thrombospondin type 1 motif, 3	chr4q13.3	12.369
COL1A1	1277	Collagen, type I, alpha 1	chr17q21.33	9.318
MMP11	4320	Matrix metalloproteinase 11 (stromelysin 3)	chr22q11.2 22q11.23	7.950
COL5A2	1290	Collagen, type V, alpha 2	chr2q14-q32	7.600
VCAN	1462	Versican	chr5q14.3	6.544
VCAN	1462	Versican	chr5q14.3	6.039
FN1	2335	Fibronectin 1	chr2q34	5.588
PTCH1	5727	Patched homolog 1 (<i>Drosophila</i>)	chr9q22.3	5.506
F2R	2149	Coagulation factor II (thrombin) receptor	chr5q13	5.348
MDK	4192	Midkine (neurite growth-promoting factor 2)	chr11p11.2	5.273
TMSB15A	11013	Thymosin beta 15a	chrXq21.33-q22.3	5.202
VCAN	1462	Versican	chr5q14.3	5.109
GPR161	23432	G protein-coupled receptor 161	chr1q24.2	5.091
SH3GL3	6457	SH3-domain GRB2-like 3	chr15q24	4.808
FAP	2191	Fibroblast activation protein, alpha	chr2q23	4.680
SHOX2	6474	Short stature homeobox 2	chr3q25-q26.1	4.665
B)				
Gene symbol	Entrez gene	Gene title	Chromosomal location	Fold change
ADIPOQ	9370	Adiponectin, C1Q and collagen domain containing	chr3q27	0.031
NR4A1	3164	Nuclear receptor subfamily 4, group A, member 1	chr12q13	0.048
PLIN1	5346	Perilipin 1	chr15q26	0.072
FABP4	2167	Fatty acid binding protein 4, adipocyte	chr8q21	0.072
IL6	3569	Interleukin 6 (interferon, beta 2)	chr7p21	0.07
SCGB2A2	4250	Secretoglobulin, family 2A, member 2	chr11q13	0.076
HSD3B1	3283	Hydroxy-delta-5-steroid dehydrogenase, 3 beta- and steroid delta-isomerase 1	chr1p13.1	0.085
ALOX15B	247	Arachidonate 15-lipoxygenase, type B	chr17p13.1	0.091
MYH11	4629	Myosin, heavy chain 11, smooth muscle	chr16p13.11	0.099
ADH1B	125	Alcohol dehydrogenase 1B (class I), beta polypeptide	chr4q21-q23	0.105
G0S2	50486	G0/G1switch 2	chr1q32.2	0.108
TCHH	7062	Trichohyalin	chr1q21.3	0.109
TIMP4	7079	TIMP metalloproteinase inhibitor 4	chr3p25	0.115
MYH11	4629	Myosin, heavy chain 11, smooth muscle	chr16p13.11	0.118
GPD1	2819	Glycerol-3-phosphate dehydrogenase 1 (soluble)	chr12q12-q13	0.119
ZBTB16	7704	Zinc finger and BTB domain containing 16	chr11q23.1	0.119
CA6	765	Carbonic anhydrase VI	chr1p36.2	0.121
FOSB	2354	FBJ murine osteosarcoma viral oncogene homolog B	chr19q13.32	0.122
PDZK1	5174	PDZ domain containing 1	chr1q21	0.138
MYH11	4629	Myosin, heavy chain 11, smooth muscle	chr16p13.11	0.142

Table VI. Transcriptionally dysregulated genes within A) putative BCC susceptibility loci, and B) within loci of known causative somatic gene mutations in BCC.

A)		
Chromosomal locus	Refs.	Mapped genes
1p36	(61)	MFAP2, STMN1, ID3 , CA6
1q42	(61)	PARP1, GNPAT
5p13.3	(55,58,62,68)	GHR, HMGCS1
5p15.33	(60,62)	PAPD7 , SRD5A1 , BASP1, LPCAT1
7q32	(60)	BPGM
9p23	(60)	ACO1
12q11-13	(60)	KRT7 , GPD1 , ITGA7 , AQP5 , KRT18 , NR4A1 , ENDOU , METTL7A , PPP1R1A
13q32	(59)	CLDN10
14q32	(69)	CHGA, CKB , DICER1
16q24.3	(52,54,56,58,68,70,71)	CDH13
19q13	(72,73)	BCAT2 , FCGBP , COX7A1 , ECH1 , ZFP36 , BLVRB , PLD3 , PPP1R15A , APOC1 , APOE , EMP3 , FOSB , ZNF135
20q11.2-12	(52,54,58,68,70,74)	ID1
B)		
Chromosomal locus	Refs.	Mapped genes
1p34-PTCH2	(75,76)	LRP8, PHC2
2q14-Gli2	(77)	MYO1B, COL5A2
5q13-RASA1	(78)	F2R, TNPO1, AGGF1, HMGCR
9q22-PTCH1	(79,80)	NFIL3 , NTRK2 , PTCH1 , FBP1
10q24-SUFU	(81)	IFIT3, PLAU, PPP1R3C
17p13-p53	(82)	ACADVL , ALOX15B , PER1 , C17orf91

DEGs found within putative BCC susceptibility loci, are annotated by chromosomal location. Bold indicates downregulated genes.

P53, a tumor suppressor protein responsible for cell cycle arrest in the presence of DNA damage has been implicated in a multitude of cancers, including BCC (9,10,36,37). Our results show that four downregulated DEGs share the same chromosomal location as p53 (Table VI), indicating that 17p13 may in fact be an important susceptibility locus for BCC. Additionally, two other DEGs confirm the importance of p53 in BCC pathogenesis. The first, CDKN1A, encodes p21, a cyclin dependent kinase inhibitor and major mediator of the p53 pathway. Because p21 is tightly regulated by p53, the downregulation of CDKN1A may indicate the presence of a mutation in the tumor suppressor gene (38). P53 also plays an important role in the regulation of MMP1, a degradative enzyme family member that breaks down the extracellular matrix during tissue development, remodeling, and repair (37). In our list of DEGs, MMP1 was upregulated. Given that p53 downregulates MMP1, this may again reflect a gene mutation. MMP1 is also important in tumor progression through its role in the stimulation of tumor-induced angiogenesis and local tissue invasion. The concomitant downregulation of TIMP4, a family member of MMP inhibitors whose down-

regulation has been associated with excessive ECM degradation (39), may also contribute to tumor growth and invasion.

Several physiological mechanisms appear to be activated in order to counteract the pathological state in BCC. Our analysis reveals an upregulation of DAPK1 (DAPK1), a candidate tumor suppressor whose mechanism includes inhibition of ERK. This upregulation affects both the Ras-MAPK and TGF- β pathways that may support tumor suppressive changes. The Ras-MAPK pathway plays an important role in many cellular functions, including proliferation, differentiation, migration and cell survival (40). Constitutive activation of this pathway, either via mutation or dysregulation, is associated with many cancers, including melanoma, breast, pancreatic, head and neck, and colon cancers (41-45). In this tightly regulated pathway, the inhibition of ERK by DAPK1 results in the downregulation of FOS and MYC, two oncogenes associated with uncontrolled proliferation and thus tumorigenesis. The TGF- β pathway is similarly involved in proliferation, differentiation, growth and cell death (46). Inhibition of ERK in this pathway allows for the upregulation of the transcription factor E2F5 (E2F5). E2F5

has an established role in the inhibition of MYC (47), therefore its upregulation may be another mechanism for tumor suppression. Further study on the role of E2F5 in BCC is warranted given recent evidence suggesting that E2F5 may contribute to tumorigenesis (48,49).

A recently published meta-analysis from our lab revealed overlapping DEGs across no more than 2 BCC microarray studies (50). We extended this analysis here with the most currently available literature and discovered that 13 DEGs overlapped across 3 studies (Table IV). Functional annotation of these genes revealed transcriptional dysregulation of processes involved in lipid/steroid metabolism and of components of the extracellular matrix. The dysregulated genes involved in lipid metabolism may point to underlying aberrations leading to BCC tumorigenesis and represent potential biomarkers for the development of BCC. To understand if transcriptional dysregulation of lipid metabolism can act as a diagnostic indicator, future studies may include linking fine-tuned time-course measurements with changes in gene expression. Also, we noted an upregulation in extracellular matrix-related genes. Previous studies have indicated that BCC samples that were less invasive typically contained a dense matrix surrounding the cells (51). It has been postulated that this stroma precludes cellular proliferation and tumor metastasis by introducing a physical barrier to migrating cells and helps explain the slow-growing properties of BCC.

Numerous genome-wide association studies have identified putative susceptibility loci that are associated with basal cell carcinoma (52-62). However, consensus risk loci have not been established and these studies do not shed light on the causal relationships between genes and phenotype. Here, we combined information from established genetic linkage studies on BCC susceptibility with gene expression data from our microarray analysis to draw insights on the development of basal cell carcinoma. We expect that subsets of genes differentially expressed in BCC are due to genetic alterations. Thus, disease associated DEGs are likely to represent an enriched pool of candidate risk genes. Moreover, we found 26 BCC associated DEGs that mapped to eight previously reported BCC susceptibility identified loci (Table VI). Four DEGs mapped to locations previously associated with BCC and pigmentation genes related to eye color, hair color, and/or skin color. The remaining DEGs mapped to putative susceptibility loci that were associated with BCC only and not pigmentation. It should be noted that none of the 26 DEGs that mapped to loci were related to pigmentation alone, indicating that any primary genetic associations are likely to be linked to tumor development.

A recent GWAS identified KRT5 as a gene of interest associated with BCC at the 12q11-13 locus (61). Our analysis revealed 9 downregulated DEGs that mapped to the 12q13 region. This pool of 9 DEGs at 12q13 warrant further study to investigate which of these represent true risk loci. Thus, the strategy of merging genetics and transcriptional datasets can be leveraged to refine the search for susceptibility loci, particularly those with functional consequence.

Our study identified chromosome 5 as a chromosome with significantly enriched DEGs. We further found four regions on chromosome 5 that might serve as transcriptional 'hot spots' for BCC. In particular, the 5p13-15.33 region overlapped with two susceptibility loci (5p13 and 5p15) that were previously identified in GWAS and linkage studies. Our study also revealed

novel chromosomal locations at the 5q11.2-14.3, 5q22.1-23.3 and 5q31-35.3 regions. 5q11 was recently identified in a GWAS as a susceptibility locus in patients with esophageal squamous cell carcinoma (63). The 5q35 region was previously associated with prostate cancer development, however, the causal genes at play were not identified (64,65). In genome-wide association and linkage studies, 5q21.1 and 5q31-33 loci were associated with atopic dermatitis (66,67). These results underscore the potential pathogenetic significance of the identified chromosomal locations, suggesting regions that may be prioritized for rigorous genetic association studies.

We expect our approach of integrating available genetic information with transcriptional data will facilitate future investigations to pinpoint susceptibility loci with greater precision to better illuminate the causative links between genetic alteration, transcriptional dysregulation, and disease initiation and progression in BCC. Taken together, such information could be used to improve on current diagnostic and prognostic modalities, and further our understanding of disease mechanisms in order to develop enriched targets for therapy.

Acknowledgements

We thank the housestaff at the Department of Dermatology, Weill-Cornell Medical College, and New York Presbyterian Hospital for help with procurement of tissue samples.

References

1. Armstrong BK and Kricger A: Skin cancer. *Dermatol Clin* 13: 583-594, 1995.
2. Rubin AI, Chen EH and Ratner D: Basal-cell carcinoma. *N Engl J Med* 353: 2262-2269, 2005.
3. Sexton M, Jones DB and Maloney ME: Histologic pattern analysis of basal cell carcinoma. Study of a series of 1039 consecutive neoplasms. *J Am Acad Dermatol* 23: 1118-1126, 1990.
4. Diepgen TL and Mahler V: The epidemiology of skin cancer. *Br J Dermatol* 146 (Suppl. 61): S1-S6, 2002.
5. Reifemberger J, Wolter M, Knobbe CB, *et al*: Somatic mutations in the PTCH, SMOH, SUFUH and TP53 genes in sporadic basal cell carcinomas. *Br J Dermatol* 152: 43-51, 2005.
6. Benjamin CL, Melnikova VO and Ananthaswamy HN: P53 protein and pathogenesis of melanoma and nonmelanoma skin cancer. *Adv Exp Med Biol* 624: 265-282, 2008.
7. De Zwaan SE and Haass NK: Genetics of basal cell carcinoma. *Australas J Dermatol* 51: 81-93, 2010.
8. Iwasaki JK, Srivastava D, Moy RL, Lin HJ and Kouba DJ: The molecular genetics underlying basal cell carcinoma pathogenesis and links to targeted therapeutics. *J Am Acad Dermatol* 66: E167-E168, 2012.
9. Lacour JP: Carcinogenesis of basal cell carcinomas: genetics and molecular mechanisms. *Br J Dermatol* 146 (Suppl 61): S17-S19, 2002.
10. Muller PA, Vousden KH and Norman JC: p53 and its mutants in tumor cell migration and invasion. *J Cell Biol* 192: 209-218, 2011.
11. Gentleman RC, Carey VJ, Bates DM, *et al*: Bioconductor: open software development for computational biology and bioinformatics. *Genome Biol* 5: R80, 2004.
12. Wilson CL and Miller CJ: Simpleaffy: a BioConductor package for Affymetrix Quality Control and data analysis. *Bioinformatics* 21: 3683-3685, 2005.
13. Smyth GK: Linear models and empirical bayes methods for assessing differential expression in microarray experiments. *Stat Appl Genet Mol Biol* 3: Article 3, 2004.
14. Benjamini Y: Controlling the false discovery rate: a practical and powerful approach to multiple testing. *J R Stat Soc Series B* 57: 289-300, 1995.
15. Eisen MB, Spellman PT, Brown PO and Botstein D: Cluster analysis and display of genome-wide expression patterns. *Proc Natl Acad Sci USA* 95: 14863-14868, 1998.

16. Huang da W, Sherman BT, Tan Q, *et al*: DAVID Bioinformatics Resources: expanded annotation database and novel algorithms to better extract biology from large gene lists. *Nucleic Acids Res* 35: W169-W175, 2007.
17. Asplund A, Gry Bjorklund M, Sundquist C, *et al*: Expression profiling of microdissected cell populations selected from basal cells in normal epidermis and basal cell carcinoma. *Br J Dermatol* 158: 527-538, 2008.
18. Howell BG, Solish N, Lu C, *et al*: Microarray profiles of human basal cell carcinoma: insights into tumor growth and behavior. *J Dermatol Sci* 39: 39-51, 2005.
19. O'Driscoll L, McMorro J, Doolan P, *et al*: Investigation of the molecular profile of basal cell carcinoma using whole genome microarrays. *Mol Cancer* 5: 74, 2006.
20. Yu M, Zloty D, Cowan B, *et al*: Superficial, nodular, and morpheiform basal-cell carcinomas exhibit distinct gene expression profiles. *J Invest Dermatol* 128: 1797-1805, 2008.
21. Nijsten T, Geluyckens E, Colpaert C and Lambert J: Peroxisome proliferator-activated receptors in squamous cell carcinoma and its precursors. *J Cutan Pathol* 32: 340-347, 2005.
22. Tachibana K, Yamasaki D, Ishimoto K and Doi T: The role of PPARs in cancer. *PPAR Res* 2008: 102737, 2008.
23. Reka AK, Goswami MT, Krishnapuram R, Standiford TJ and Keshamouni VG: Molecular cross-regulation between PPAR-gamma and other signaling pathways: implications for lung cancer therapy. *Lung Cancer* 72: 154-159, 2011.
24. Sarraf P, Mueller E, Jones D, *et al*: Differentiation and reversal of malignant changes in colon cancer through PPARgamma. *Nat Med* 4: 1046-1052, 1998.
25. Guan YF, Zhang YH, Breyer RM, Davis L and Breyer MD: Expression of peroxisome proliferator-activated receptor gamma (PPARgamma) in human transitional bladder cancer and its role in inducing cell death. *Neoplasia* 1: 330-339, 1999.
26. Mossner R, Schulz U, Kruger U, *et al*: Agonists of peroxisome proliferator-activated receptor gamma inhibit cell growth in malignant melanoma. *J Invest Dermatol* 119: 576-582, 2002.
27. Petta E, Sotiropoulou-Bonikou G, Kourelis K, Melachrinou M and Bonikos DS: Differential expression and cross-talk of peroxisome proliferator-activated receptor gamma and retinoid-X receptor alpha in urothelial carcinomas of the bladder. *J BUON* 15: 740-745, 2010.
28. Pancione M, Forte N, Sabatino L, *et al*: Reduced beta-catenin and peroxisome proliferator-activated receptor-gamma expression levels are associated with colorectal cancer metastatic progression: correlation with tumor-associated macrophages, cyclooxygenase 2, and patient outcome. *Hum Pathol* 40: 714-725, 2009.
29. Mueller E, Sarraf P, Tontonoz P, *et al*: Terminal differentiation of human breast cancer through PPAR gamma. *Mol Cell* 1: 465-470, 1998.
30. Yao L, Liu F, Sun L, *et al*: Upregulation of PPARgamma in tissue with gastric carcinoma. *Hybridoma (Larchmt)* 29: 341-343, 2010.
31. Wang W, Wang R, Zhang Z, Li D and Yut Y: Enhanced PPAR-gamma expression may correlate with the development of Barrett's esophagus and esophageal adenocarcinoma. *Oncol Res* 19: 141-147, 2011.
32. Li M, Lee TW, Mok TS, Warner TD, Yim AP and Chen GG: Activation of peroxisome proliferator-activated receptor-gamma by troglitazone (TGZ) inhibits human lung cell growth. *J Cell Biochem* 96: 760-774, 2005.
33. Boiteux G, Lascombe I, Roche E, *et al*: A-FABP, a candidate progression marker of human transitional cell carcinoma of the bladder, is differentially regulated by PPAR in urothelial cancer cells. *Int J Cancer* 124: 1820-1828, 2009.
34. Storch J and Thumser AE: Tissue-specific functions in the fatty acid-binding protein family. *J Biol Chem* 285: 32679-32683, 2010.
35. Wetmore C: Sonic hedgehog in normal and neoplastic proliferation: insight gained from human tumors and animal models. *Curr Opin Genet Dev* 13: 34-42, 2003.
36. Green DR and Kroemer G: Cytoplasmic functions of the tumour suppressor p53. *Nature* 458: 1127-1130, 2009.
37. Sun Y, Zeng XR, Wenger L, Firestein GS and Cheung HS: P53 down-regulates matrix metalloproteinase-1 by targeting the communications between AP-1 and the basal transcription complex. *J Cell Biochem* 92: 258-269, 2004.
38. Jung YS, Qian Y and Chen X: Examination of the expanding pathways for the regulation of p21 expression and activity. *Cell Signal* 22: 1003-1012, 2010.
39. Tanaka K, Iwamoto Y, Ito Y, *et al*: Cyclic AMP-regulated synthesis of the tissue inhibitors of metalloproteinases suppresses the invasive potential of the human fibrosarcoma cell line HT1080. *Cancer Res* 55: 2927-2935, 1995.
40. Tartaglia M and Gelb BD: Disorders of dysregulated signal traffic through the RAS-MAPK pathway: phenotypic spectrum and molecular mechanisms. *Ann N Y Acad Sci* 1214: 99-121, 2010.
41. Dunn KL, Espino PS, Drobnic B, He S and Davie JR: The Ras-MAPK signal transduction pathway, cancer and chromatin remodeling. *Biochem Cell Biol* 83: 1-14, 2005.
42. Yang D, Tao J, Li L, *et al*: RasGRP3, a Ras activator, contributes to signaling and the tumorigenic phenotype in human melanoma. *Oncogene* 30: 4590-600, 2011.
43. Mathiasen DP, Egebjerg C, Andersen SH, *et al*: Identification of a c-Jun N-terminal kinase-2-dependent signal amplification cascade that regulates c-Myc levels in ras transformation. *Oncogene* 31: 390-401, 2012.
44. Shi XH, Liang ZY, Ren XY and Liu TH: Combined silencing of K-ras and Akt2 oncogenes achieves synergistic effects in inhibiting pancreatic cancer cell growth in vitro and in vivo. *Cancer Gene Ther* 16: 227-236, 2009.
45. Rauch J, Moran-Jones K, Albrecht V, *et al*: c-Myc regulates RNA splicing of the A-Raf kinase and its activation of the ERK pathway. *Cancer Res* 71: 4664-4674, 2011.
46. Su E, Han X and Jiang G: The transforming growth factor beta 1/SMAD signaling pathway involved in human chronic myeloid leukemia. *Tumori* 96: 659-666, 2010.
47. Chen CR, Kang Y, Siegel PM and Massague J: E2F4/5 and p107 as Smad cofactors linking the TGFbeta receptor to c-myc repression. *Cell* 110: 19-32, 2002.
48. Jiang Y, Yim SH, Xu HD, *et al*: A potential oncogenic role of the commonly observed E2F5 overexpression in hepatocellular carcinoma. *World J Gastroenterol* 17: 470-477, 2011.
49. Polanowska J, Le Cam L, Orsetti B, *et al*: Human E2F5 gene is oncogenic in primary rodent cells and is amplified in human breast tumors. *Genes Chromosomes Cancer* 28: 126-130, 2000.
50. Van Haren R, Feldman D and Sinha AA: Systematic comparison of nonmelanoma skin cancer microarray datasets reveals lack of consensus genes. *Br J Dermatol* 161: 1278-1287, 2009.
51. Tanaka K, Iyama K, Kitaoka M, *et al*: Differential expression of alpha 1(IV), alpha 2(IV), alpha 5(IV) and alpha 6(IV) collagen chains in the basement membrane of basal cell carcinoma. *Histochem J* 29: 563-570, 1997.
52. Bishop DT, Demenais F, Iles MM, *et al*: Genome-wide association study identifies three loci associated with melanoma risk. *Nat Genet* 41: 920-925, 2009.
53. Gerstenblith MR, Shi J and Landi MT: Genome-wide association studies of pigmentation and skin cancer: a review and meta-analysis. *Pigment Cell Melanoma Res* 23: 587-606, 2010.
54. Gudbjartsson DF, Sulem P, Stacey SN, *et al*: ASIP and TYR pigmentation variants associate with cutaneous melanoma and basal cell carcinoma. *Nat Genet* 40: 886-891, 2008.
55. Han J, Kraft P, Nan H, *et al*: A genome-wide association study identifies novel alleles associated with hair color and skin pigmentation. *PLoS Genet* 4: e1000074, 2008.
56. Han J, Qureshi AA, Prescott J, *et al*: A prospective study of telomere length and the risk of skin cancer. *J Invest Dermatol* 129: 415-421, 2009.
57. Liboutet M, Portela M, Delestaing G, *et al*: MC1R and PTCH gene polymorphism in French patients with basal cell carcinomas. *J Invest Dermatol* 126: 1510-1517, 2006.
58. Nan H, Kraft P, Hunter DJ and Han J: Genetic variants in pigmentation genes, pigmentary phenotypes, and risk of skin cancer in Caucasians. *Int J Cancer* 125: 909-917, 2009.
59. Nan H, Xu M, Kraft P, *et al*: Genome-wide association study identifies novel alleles associated with risk of cutaneous basal cell carcinoma and squamous cell carcinoma. *Hum Mol Genet* 20: 3718-3724, 2011.
60. Rafnar T, Sulem P, Stacey SN, *et al*: Sequence variants at the TERT-CLPTM1L locus associate with many cancer types. *Nat Genet* 41: 221-227, 2009.
61. Stacey SN, Gudbjartsson DF, Sulem P, *et al*: Common variants on 1p36 and 1q42 are associated with cutaneous basal cell carcinoma but not with melanoma or pigmentation traits. *Nat Genet* 40: 1313-1318, 2008.
62. Stacey SN, Sulem P, Masson G, *et al*: New common variants affecting susceptibility to basal cell carcinoma. *Nat Genet* 41: 909-914, 2009.
63. Wu C, Hu Z, He Z, *et al*: Genome-wide association study identifies three new susceptibility loci for esophageal squamous-cell carcinoma in Chinese populations. *Nat Genet* 43: 679-684, 2011.
64. Christensen GB, Baffoe-Bonnie AB, George A, *et al*: Genome-wide linkage analysis of 1,233 prostate cancer pedigrees from the International Consortium for Prostate Cancer Genetics using novel sumLINK and sumLOD analyses. *Prostate* 70: 735-744, 2010.

65. Xu J, Dimitrov L, Chang BL, *et al*: A combined genomewide linkage scan of 1,233 families for prostate cancer-susceptibility genes conducted by the international consortium for prostate cancer genetics. *Am J Hum Genet* 77: 219-229, 2005.
66. Sun LD, Xiao FL, Li Y, *et al*: Genome-wide association study identifies two new susceptibility loci for atopic dermatitis in the Chinese Han population. *Nat Genet* 43: 690-694, 2011.
67. Beyer K, Nickel R, Freidhoff L, *et al*: Association and linkage of atopic dermatitis with chromosome 13q12-14 and 5q31-33 markers. *J Invest Dermatol* 115: 906-908, 2000.
68. Duffy DL, Zhao ZZ, Sturm RA, Hayward NK, Martin NG and Montgomery GW: Multiple pigmentation gene polymorphisms account for a substantial proportion of risk of cutaneous malignant melanoma. *J Invest Dermatol* 130: 520-528, 2010.
69. Han J, Colditz GA, Samson LD and Hunter DJ: Polymorphisms in DNA double-strand break repair genes and skin cancer risk. *Cancer Res* 64: 3009-3013, 2004.
70. Sulem P, Gudbjartsson DF, Stacey SN, *et al*: Two newly identified genetic determinants of pigmentation in Europeans. *Nat Genet* 40: 835-837, 2008.
71. Sulem P, Gudbjartsson DF, Stacey SN, *et al*: Genetic determinants of hair, eye and skin pigmentation in Europeans. *Nat Genet* 39: 1443-1452, 2007.
72. Han J, Hankinson SE, Colditz GA and Hunter DJ: Genetic variation in XRCC1, sun exposure, and risk of skin cancer. *Br J Cancer* 91: 1604-1609, 2004.
73. Kang SY, Lee KG, Lee W, *et al*: Polymorphisms in the DNA repair gene XRCC1 associated with basal cell carcinoma and squamous cell carcinoma of the skin in a Korean population. *Cancer Sci* 98: 716-720, 2007.
74. Brown KM, Macgregor S, Montgomery GW, *et al*: Common sequence variants on 20q11.22 confer melanoma susceptibility. *Nat Genet* 40: 838-840, 2008.
75. Smyth I, Narang MA, Evans T, *et al*: Isolation and characterization of human patched 2 (PTCH2), a putative tumour suppressor gene in basal cell carcinoma and medulloblastoma on chromosome 1p32. *Hum Mol Genet* 8: 291-297, 1999.
76. Fan Z, Li J, Du J, *et al*: A missense mutation in PTCH2 underlies dominantly inherited NBCCS in a Chinese family. *J Med Genet* 45: 303-308, 2008.
77. Grachtchouk M, Mo R, Yu S, *et al*: Basal cell carcinomas in mice overexpressing Gli2 in skin. *Nat Genet* 24: 216-217, 2000.
78. Friedman E, Gejman PV, Martin GA and McCormick F: Non-sense mutations in the C-terminal SH2 region of the GTPase activating protein (GAP) gene in human tumours. *Nat Genet* 5: 242-247, 1993.
79. Hahn H, Wicking C, Zaphiropoulos PG, *et al*: Mutations of the human homolog of *Drosophila* patched in the nevoid basal cell carcinoma syndrome. *Cell* 85: 841-851, 1996.
80. Aszterbaum M, Epstein J, Oro A, *et al*: Ultraviolet and ionizing radiation enhance the growth of BCCs and trichoblastomas in patched heterozygous knockout mice. *Nat Med* 5: 1285-1291, 1999.
81. Svard J, Heby-Henricson K, Persson-Lek M, *et al*: Genetic elimination of Suppressor of fused reveals an essential repressor function in the mammalian Hedgehog signaling pathway. *Dev Cell* 10: 187-197, 2006.
82. Ling G, Ahmadian A, Persson A, *et al*: PATCHED and p53 gene alterations in sporadic and hereditary basal cell cancer. *Oncogene* 20: 7770-7778, 2001.